JEE Journal of Ecological Engineering

*Journal of Ecological Engineering*, 2026, 27(8), 202–218
https://doi.org/10.12911/22998993/220461
ISSN 2299–8993, License CC-BY 4.0

Received: 2026.02.27
Accepted: 2026.05.08
Published: 2026.07.01

# From effluent to energy: Maximizing olive mill wastewater bioconversion and bioelectricity generation in microbial fuel cells

Mohammed Zine[1*], Fouzia Allali[1], Siham El Mazouzi[2], Noureddine Touach[1], Latifa Tajounte[1], Kaoutar Kara[1], Behnam Taidi[3], El Mostapha Lotfi[1]

[1] Laboratory of Spectroscopy, Molecular. Modeling, Materials, Nanomaterials, Water and Environment, Environmental Materials Team, ENSAM, Mohammed V University in Rabat, Morocco
[2] Physical Chemistry of Materials Laboratory, Ben M'sick Faculty of Sciences, Hassan II University, Boulevard Cdt Driss El Harti B.P 7955, Casablanca, Morocco
[3] Laboratory of Process Engineering and Materials, Centrale Supelec, Paris, France
* Corresponding author's e-mail: mohammedzine34@gmail.com

## ABSTRACT

The Moroccan olive oil sector produces large volumes of olive mill wastewater (OMW), a highly polluting effluent rich in polyphenols and organic load (chemical oxygen demand: COD). This study explores an integrated solution using microbial fuel cells (MFCs) to simultaneously remediate OMW and generate bioelectricity. We investigated how initial phenolic concentration influences bioelectrochemical performance using two distinct OMW samples (OMW1 and OMW4). Remarkably, power densities reached 1028 $mW \cdot m^{-3}$ and 1200 $mW \cdot m^{-3}$ , respectively. Corresponding phenolic reductions were 56% for OMW1 (1 $g \cdot L^{-1}$ and 0.438 $g \cdot L^{-1}$ as initial,final concentrations respectively) and 70% for OMW4 (4 $g \cdot L^{-1}$ and 1186 $g \cdot L^{-1}$ as initial and final concentrations respectively), while COD removal achieved 52% and 76%, highlighting a direct link between substrate richness and system efficiency. Additionally, MFCs demonstrated substantial heavy metal removal (30–97%), confirming their multifunctional potential. These findings underscore the capacity of MFCs to convert a high-impact pollutant into renewable energy, offering a sustainable pathway for olive industry waste management in Mediterranean regions.The originality of the present study is based,firstly,on the systematic comparative investigation of two OMW samples in MFC treatment. Thereby, the impact of the complex OMW matrix, especially that of inhibitory phenolic compounds, is effectively decoupled from the system performance. Secondly, bioelectrochemical performance (delivering high power densities, COD and heavy metals removal rates) was reached in a short experimental time (5 days).

**Keywords:** COD removal rate, microbial fuel cells, olive mill wastewater, bioelectricity generation, phenolic compounds removal rate, heavy metals removal rate.

## INTRODUCTION

Agro-industrial production has evolved exponentially due to rising global demand, which has generated a huge amount of organic waste, creating a significant environmental problem (Shah et al., 2025; Awasthi et al., 2022; Choe et al., 2022). The FAO estimates that about 1.3 billion tons of food are wasted every year, and it is predicted that global waste generation will reach 3.4 billion tons per year by 2050 (Kaza et al., 2018; Kilemile et al., 2025). The widespread neglect of solid waste management is a global issue with far-reaching implications for environmental contamination, social cohesion, and long-term economic sustainability (Ferronato et al., 2019; Abubakar et al., 2022; De Souza Melaré et al., 2017). In response, intensive research has focused on valorizing organic waste into biogas, compost, or bioelectricity as a means of transforming it into a resource (Wainaina et al., 2020; Ishita et al., 2020).

Among these industries, olive oil production is a cornerstone of the Mediterranean economy but also a major source of highly polluting

effluent. Close to 97% of global production is located in Spain, Italy, Greece, and Morocco (Djeziri et al., 2023). Indeed, the traditional three-phase extraction process consumes between 80 and 120 L of water per 100 kg of olives, generating huge volumes of olive mill wastewater (OMW) (Dich et al., 2025). This effluent has an intense dark color and an unpleasant odor, along with an extremely high organic load, with chemical oxygen demand (COD) values ranging from 31 to 200 g $L^{-1}$ (Agabo-García et al., 2023). Among the most worrying environmental issues linked to OMW is the elevated concentration of phenolic compounds, which are toxic, phytotoxic, and recalcitrant to biodegradation, making them serious pollutants of water and soil (Athanasiadis et al., 2023). The phenolic compounds found in OMWs are derived from olive fruits (naturally occurring phenolic compounds found in olive pulp, skin, and stone). Among these molecules: hydroxytyrosol, tyrosol, oleuropein, caffeic acid, p-coumaric acid and verbascoside. The varying amounts of these compounds in OMWs are due to olive variety and harvest timing (Solomakou et al., 2021).

Current OMW management practices, such as storage in evaporation ponds, are cost-effective but often result in soil clogging and groundwater contamination (Jarboui et al., 2023). Conventional wastewater treatments in olive oil production consist of sequential processes tailored to the high-strength and phytotoxic nature of OMW. Treatment typically begins with preliminary screening and dissolved air flotation (DAF), which remove coarse solids, lipids, and grease from the influent. This may be followed by an important physico-chemical step—often coagulation-flocculation—to reduce the organic load and lower the concentration of phenolic compounds, facilitating their separation by sedimentation or flotation. The biological step then often treats the remaining high COD through anaerobic digestion with biogas recovery (Vaz et al., 2025). However, these conventional treatments have serious limitations: they produce large amounts of toxic chemical sludge, creating a secondary disposal problem, and biological treatment is frequently hindered by the residual toxicity of polyphenols, leading to instability in bioreactors and requiring long acclimatization periods.Advanced oxidation processes (AOPs) and membrane-based systems have shown higher efficiency but are energy-intensive and expensive, limiting large-scale application (Mannaf et al., 2025; Ahmed et al., 2025). Aerobic and anaerobic treatments are cost-effective options, achieving up to 90% COD and phenolic compound removal in optimized systems. In this context, microbial fuel cells (MFCs) have emerged as a promising technology that can effectively treat wastewater while recovering energy (Jafary et al., 2026; Yaqoob et al., 2023). MFCs employ electroactive bacteria to oxidize organic substrates at the anode, generating electrons that travel through an external circuit to the cathode, where they combine with protons and oxygen to form water, thereby producing an electric current (Touach et al., 2023; Touach et al., 2017; Hitar et al., 2024; Benzaouak et al., 2018; Rehman et al., 2025).

$$O_2 + 4H^+ + 4e^- \rightarrow 2H_2O \ (E_0 = 1.23 \text{ V}) \quad (1)$$

However, material costs and performance variability – particularly in the case of complex, inhibitory substrates such as OMW – hinder the scalability of MFCs. Various electrode materials, including those made of $TiO_2$ and lithium-based perovskites, have been tested for improved electron transfer and system efficiency (Touach et al., 2017; Hitar et al., 2024; Benzaouak et al., 2018; Rehman et al., 2025; Ma et al., 2021). A review (Ucar et al., 2017) corroborates this research direction, noting that the development of affordable, high-surface-area, biocompatible anodes is crucial for enhancing electron transfer kinetics and enriching robust electroactive biofilms capable of withstanding such inhibitory environments (Ucar et al., 2017). OMW poses a particular challenge for biological treatment due to its elevated concentration of phenolic compounds and long-chain fatty acids, which exert antimicrobial effects by altering cell membrane permeability and morphology (Palatsi et al., 2009). To minimize inhibition, dilution strategies are often employed (Bouigua et al., 2024). Nevertheless, phenolic compounds remain persistent and are classified as priority pollutants because of their toxicity, carbolic odor, and adverse effects on aquatic life even at low concentrations (Gucbilmez, 2022).

Two single-chamber MFCs, equipped with graphite and $MnO_2$ (carbon cloth composite) electrodes and a Nafion proton exchange membrane (PEM), were operated using two OMW samples with distinct initial phenolic concentrations. Graphite was selected as the anode and $MnO_2$ as the air-cathode based on their respective abilities to support the crucial bioredox

reactions at both electrodes, while maintaining operational stability with economic viability – an important consideration for wastewater treatment. Graphite, in various forms such as rods, felt, or granules, possesses all the characteristics required for an anode material. It has very good electrical conductivity, allowing for efficient electron transfer from respiring microbes to the current collector. Additionally, its chemical stability under anaerobic conditions in complex wastewater prevents corrosion and fouling, while its nontoxic nature and surface roughness enable stable colonization and growth of exoelectrogenic bacteria, such as *Geobacter* and *Shewanella* spp. (Chen et al., 2020). Due to its properties, $MnO_2$ is becoming one of the leading non-precious metal catalysts because of its excellent electrocatalytic properties, natural abundance, and low environmental toxicity. $MnO_2$ enables a multi-electron transfer pathway for the oxygen reduction reaction (ORR) and significantly enhances cathodic reaction kinetics compared to plain carbon cathodes. Its stability under neutral pH and relative insensitivity to common impurities make it a robust and economically viable catalyst material, which directly contributes to the sustainability and economic feasibility of large-scale MFC technology for wastewater treatment.

Over a five-day experimental period, key parameters – including voltage, current, and power densities, phenolic compound removal (followed by HPLC-UV), COD reduction, and heavy metal elimination – were monitored to assess the relationship between OMW composition and bioelectrogenic performance. The results provide insights into the feasibility of using MFCs as a sustainable solution for converting OMW from effluent to energy.This work offers an original investigation into the effectiveness of single-chamber MFCs for the simultaneous treatment and bioenergy recovery from OMW with distinctly different pollutant loads. The novelty of the present study lies in the systematic comparative investigation of two OMW samples (OMW1 and OMW4) in MFC treatment using cost-effective $MnO_2$-carbon cloth composite cathode-equipped MFCs. Through this approach, the impact of the complex OMW matrix, particularly that of inhibitory phenolic compounds, was effectively decoupled from the system, and bioelectrogenic performance was achieved over a short operating period (five days).

## MATERIALS AND METHODS

### MFCs configuration and operational protocol

Figure 1 shows a schematic illustration of the MFC setup employed in this investigation. The reactor consisted of a 250 mL double-jacket glass bottle to regulate temperature (25 °C). Polytetrafluoroethylene (PTFE; Sigma-Aldrich, Spain), which served as the binder, was combined with $MnO_2$ (99%, Sarreguemnes) as catalyst at a mass ratio of 1:9 before being mechanically compressed to spread 60 mg of the resulting mixture evenly across a circular piece of carbon fabric with a 1.5 $cm^2$ diameter (Fuel Cell Store, USA). The anode was composed of a graphite rod (Graphite Store, USA) connected to the cathode terminal by a 1 kΩ resistor and made of graphite granules measuring 2 to 6 mm in diameter.Two reactors were fed with 225 mL of two different OMW samples. A first series of experiments was conducted using an OMW sample with a phenolic concentration of 1 g $L^{-1}$ (OMW1), and a second series was conducted using an OMW sample with a phenolic concentration of 4 g $L^{-1}$ (OMW4). Table 1 shows the physicochemical characteristics of the two OMW samples. Chemical oxygen demand (COD) was determined according to the APHA protocol (Larrosa-Guerrero et al., 2010) using a Spectroquant Nova 30 spectrophotometer (Merck, Germany).Conductivity was determined using a conductimeter Orion Star A212 (NF T 90-031). Total and volatile solids (TS, VS) were quantified employing a gravimetric analysis (EPA

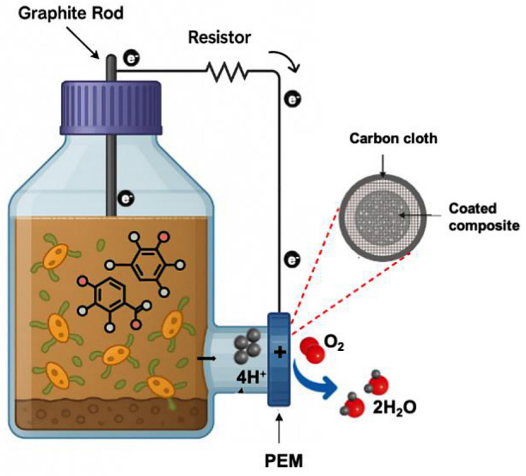


**Figure 1.** MFC's operating concept depicted schematically

**Table 1.** Physicochemical characteristics of the two OMW samples

| Sample | COD ($mg \cdot L^{-1}$) | pH | $BOD_5$ ($mg \cdot L^{-1}$) | Phenolic concentrations ($mg \cdot L^{-1}$) | Conductivity ($\mu S \cdot cm^{-1}$) | Total solids ($g \cdot L^{-1}$) | Volatile solids ($g \cdot L^{-1}$) | Temperature (°C) |
|---|---|---|---|---|---|---|---|---|
| OMW1 | 22550 | 4.67 | 19765 | 1000 | 8.2 | 28.4 | 22.1 | 25 |
| OMW4 | 43750 | 4.93 | 38263 | 4000 | 12.5 | 52.6 | 41.3 | 25 |

**Note:** COD – chemical oxygen demand, $BOD_5$ – biochemical oxygen demand.

Method 160.2 and Standard Methods 208 E). Metal species were determined by inductively coupled plasma–mass spectrometry (ICP–MS) performed using an Agilent 7500ce ICP–MS (Agilent Technologies, Santa Clara, CA, USA) equipped with an autosampler (ASX-510, Cetac Technologies Inc., Omaha, NE, USA).

Polarization and power density curves were obtained by adjusting the external resistance (11–0.9 MΩ), allowing 15 min at each resistance for stabilization.Then, the voltage was measured. Current density (I) and power density (P) were calculated using the external resistance (R), anode electrode volume ($V_{an}$), and current (I'). Voltage (U) was measured in volts (V), current density in ($mA.m^{-3}$), and power density in ($mW.m^{-3}$) (Yaqoob et al., 2023). Power density was normalized to the electrode volume (0.125 L = $1.25 \times 10^{-4}$ $m^3$) and was computed as $P = U^2/(R.V_{an})$, and current density (I) as $I = I'/V_{an} = U/(R.V_{an})$. The voltage potential across the anode and cathode was measured twice daily for each reactor using a digital multimeter (ST 9905). The corresponding current was then determined using Ohm's law.

## Electrochemical characterization

The working anode electrode was immersed in the test solution (OMW1 and OMW4) for 45 minutes to reach its stable potential. Cyclic voltammetry spectra were acquired in the potential range of –2500 to 2500 mV relative to the reference electrode, with a scan rate of 1 $mV.s^{-1}$. This immersion period facilitated comprehensive interaction between the working electrode and the solution constituents, ensuring the establishment of an electrochemical equilibrium state and a stable electrochemical potential at the working electrode. This selection of potential range and scan rate is common in electrochemical studies, as it enables precise characterization of the electrochemical reactions occurring at the electrode–solution interface.

## Phenolic compounds quantification

The Folin-Ciocalteu method was employed to determine the total phenolic content of each OMW sample. After 90 minutes of incubation at room temperature, 0.5 mL of Folin–Ciocalteu reagent and 4 mL of 1 M sodium carbonate ($Na_2CO_3$) were added to 0.1 mL of the OMW sample. Using a UV-visible spectrophotometer, the absorbance was measured at 760 nm against a blank, extract-free background. A parallel preparation of a standard range based on gallic acid was performed under identical conditions to quantify total phenolic compounds. A mother solution (1 g $L^{-1}$) of pure gallic acid standard was prepared and diluted to various concentrations (100 to 500 mg $L^{-1}$) to establish the linearity range. The results were expressed as milligrams of extract or micrograms of gallic acid equivalents (µg GAE $mg^{-1}$ of sample or g $L^{-1}$). Two separate analyses were performed (Gueboudji et al., 2021). HPLC-UV with a reversed-phase LICHROSPHER 100 RP 18 Endcapped column (BISCHOFF Chromatography) C18 (250 × 4.6 mm, 5 µm) was employed to separate the phenolic components from each OMW sample. For all phenolics, peak areas were measured at 280 nm. The identification of these compounds was achieved by comparing their retention times to those of the injected reference solution under the same operating conditions. In addition, samples were spiked to confirm peak identification. Quantification was performed using peak area and internal standard calibration.

## Coulombic efficiency determination

Coulombic efficiency (CE) represents the fraction of electrons recovered as electrical current from the total electrons available in the degraded substrate(COD reduction) (Chen et al., 2021).

$$CE\ (\%) = \left(\frac{Qactual}{Qth}\right) \times 100 =$$

$$= \frac{M(O_2) \cdot \int_0^t I \cdot dt}{F \cdot b \cdot V_{an} \cdot \Delta COD} \times 100 =$$

$$= \frac{\int_0^t I \cdot dt}{F \cdot b \cdot V_{an} \cdot \Delta S} \times 100 \qquad (2)$$

where: $F$ – Faraday's constant (96,485 C mol$^{-1}$), $b$ – number of electrons per mole of oxygen (4), $V_{an}$ – electrode volume (L), $M(O_2)$ – molecular weight of oxygen (32 g), $Q_{actual}$ – actual total coulombs transferred (C), $Q_{th}$ – theorical total coulombs transferred (C), $\Delta S = \Delta COD / M(O_2)$.

### Kinetic modeling and energy analysis

A kinetic model was developed focusing on substrate degradation (phenolic compounds and COD) and bioelectrogenic activity. Since the experimental duration is five days, first-order kinetics can be employed, which is standard for describing pollutant removal in bioelectrochemical systems under non-inhibitory or limited-inhibitory conditions.An energy analysis was also performed for both OMW1 and OMW4 treatment (Akatah and Bariture., 2023).

## RESULTS AND DISCUSSIONS

### Electrode characterization

Cyclic voltammetry (CV) technique was used to study the electrochemical behavior at the electrode surface and at the electrode-solution interface using either OMW1 or OMW4 as the medium. Figures 2a and 2b display the voltammograms of the $MnO_2$ obtained with the two OMW solutions at 100 mV.s$^{-1}$ after one and three days of operation. The results reveal that the intensity of redox current rises with operational time, consistent with previously reported findings in the literature (Yaqoob et al., 2021).

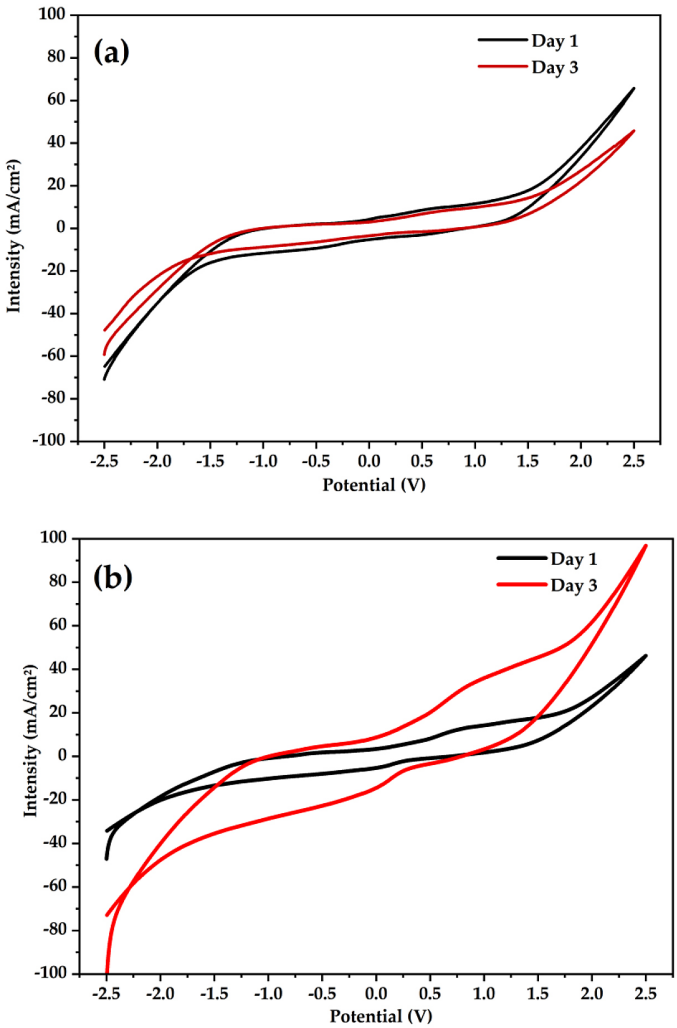


**Figure 2.** Cyclic voltammograms for MFC system with (a) OMW1 and (b) OMW4 after 1 and 3 days of operation

Additionally, the $MnO_2$-based electrode exhibited a larger electroactive area under OMW4 compared to OMW1. This phenomenon can be ascribed to the higher ionic conductivity and buffering capacity of OMW4 that eliminates any local pH gradient occurring in the electrode surface. The higher oxidation and reduction activity in the MFC system can be associated with dissolved oxygen, which acts in two steps. Oxygen reacts through a four-electron reduction pathway at the cathode ($O_2 + 4H^+ + 4e^- \rightarrow 2H_2O$). On the other hand, the oxygen-active sites on the $MnO_2$ serve for oxidation of organic matter (Wen et al., 2021). The electrons supplied from the organic substrate, mainly composed of phenolic compounds, are donated to the $MnO_2$ surface through dehydrogenation, resulting in the formation of intermediates that are further oxidized to form $CO_2$ and $H_2O$ (Yaqoob et al., 2023).

As time progresses, the exoelectrogenic bacteria attached to the electrode produce outer membrane c-type cytochromes and pili (or nanowires) that allow for the direct extracellular electron transfer (EET) to $MnO_2$, thus eliminating the need for any diffusion-based mediators. The EET process allows for reduced overpotentials, which leads to higher potential values (Torres et al., 2010). Collectively, these mechanistic insights demonstrate that the MFC process has great potential to meet both goals of OMW treatment and power generation.

## Electricity generation performances of MFCs in disposing OMW

The polarization curve is constructed by measuring how the system's voltage changes with current density. This variation is evaluated by connecting the system to different external resistances, enabling a range of voltage–current responses to be recorded and the accuracy of the obtained curve to be validated (Watson et al., 2011). The polarization curves and power density profiles of the closed-circuit air–composite MFC cathodes, operated with different OMW samples, are presented in Figure 3. The V(I) characteristic curves

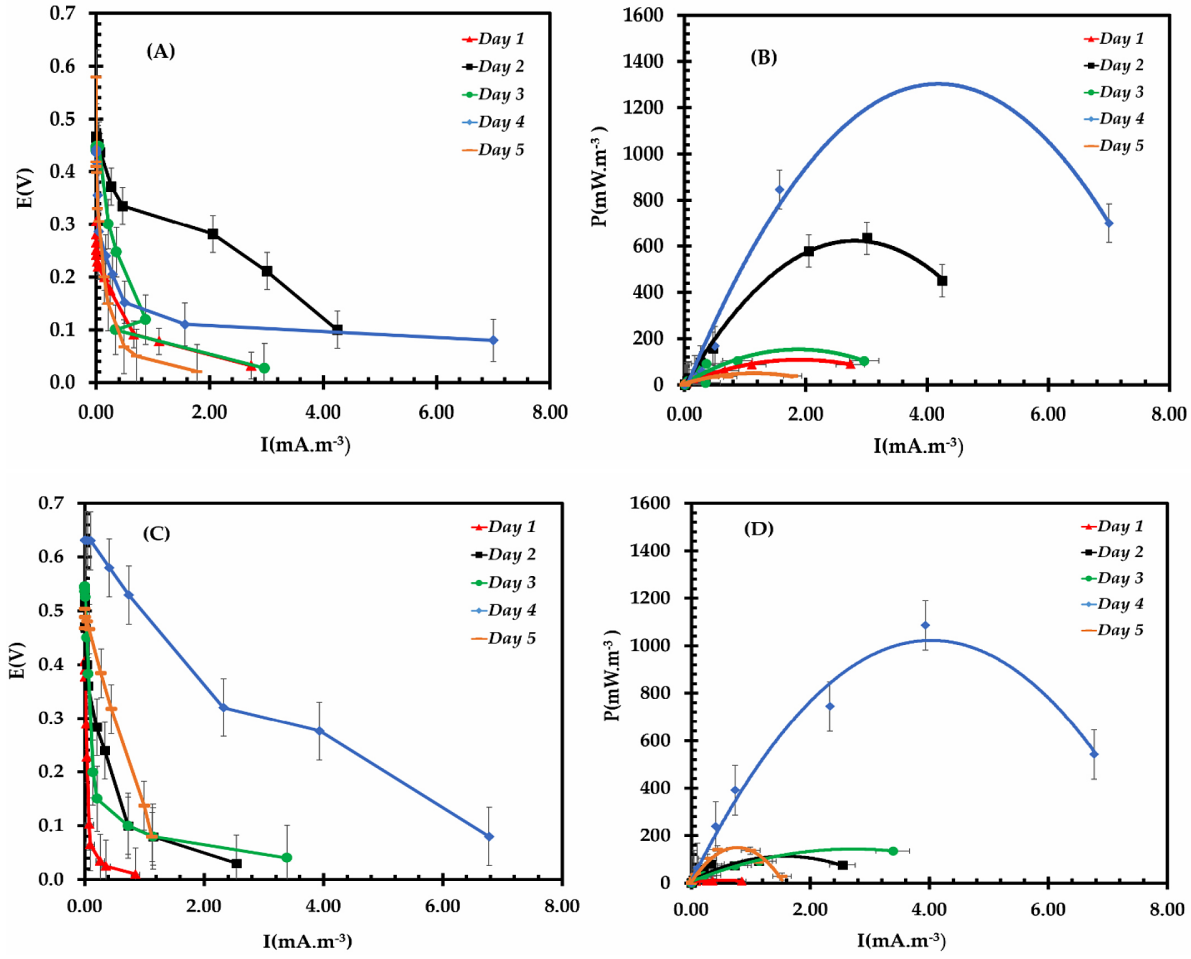


**Figure 3.** Polarization curve and power density in disposing OMW: OMW4 (A,B) and OMW1 (C,D)

obtained for MFC operation illustrate the regions where different types of losses limit the effective current output. In general, polarization curves exhibit three main regions: (i) an initial sharp voltage drop, (ii) a nearly linear decline in voltage with current, and (iii) a final steep decrease in voltage (Khabirul Islam et al., 2023; Choudhury et al., 2022). Each of these regions corresponds to a specific type of loss. Activation losses are associated with the energy needed to initiate the electrochemical reactions at the electrode surface. Charge transfer losses originate from limitations in electron and ion transport between the electrodes and the electrolyte. Ohmic losses, on the other hand, are due to the internal resistance that opposes current flow within the MFC system. A clear understanding of these losses and their combined effects is essential for improving the design and enhancing the overall performance of MFCs. According to the results presented in the figure, the MFC using a composite cathode with OMW1 and OMW4 exhibited electrocatalytic performance within the three characteristic loss domains during five days of operation. These results indicate that the maximum current density was reached on the fourth day of operation for both OMW4 and OMW1 samples, with values of 7.00 $mA.m^{-3}$ and 7.20 $mA.m^{-3}$, respectively. This trend suggests that the electrocatalytic activity of the composite cathode reaches its optimum after a few days of operation, before tending toward a stabilization or decrease phase.Power density is considered a critical indicator of MFC performance, as it represents the electrical output generated per unit of electrode surface area or reactor volume. The bell-shaped power density profiles are generally associated with the metabolic activity of exoelectrogenic microorganisms and the related redox processes occurring inside the MFC (Yoon et al., 2007). In the studied systems, both MFC-OMW1 and MFC-OMW4 exhibited notable power density values. Similarly, a clear increase was observed during the initial days of operation, reaching 1 $mW.m^{-3}$ for OMW1 and 150 $mW.m^{-3}$ for OMW4. The power density reached its maximum on the fourth day, followed by a decline on the fifth day, reflecting the dynamic evolution of electrocatalytic performance over time. This finding is consistent with the power density data in Figure 4, showing that MFC-OMW4 produced considerably higher values compared to MFC-OMW1, reaching 1200 $mW.m^{-3}$ and 1028 $mW.m^{-3}$, respectively.

The power densities obtained in this work were in the range of 1028 $mW.m^{-3}$ for OMW1 and 1200 $mW.m^{-3}$ for OMW4. These power densities compare well with or even surpass the recent reports on the bioelectricity production in MFCs using OMW. Antonopoulou et al. (2023) utilized a continuous three-air cathode single-chamber MFC fed with centrifuged OMW. The power densities obtained were in the range from 0.7 to 2 $W.m^{-3}$, corresponding to 700 $mW.m^{-3}$ to 2000 $mW.m^{-3}$. These results were obtained in the same range of performance as the integrated MFC system presented in this work. Contrary to our results,Güneş et al.(2025) utilized soil-based MFC for OMW treatment. The maximum power density obtained was 498.26 $mW.m^{-2}$. The calculated power density was lower compared to the power density obtained in this work. The main reason for this might be the use of soil in the reactor. Moreover, Pugazhendi and Jamal (2023)

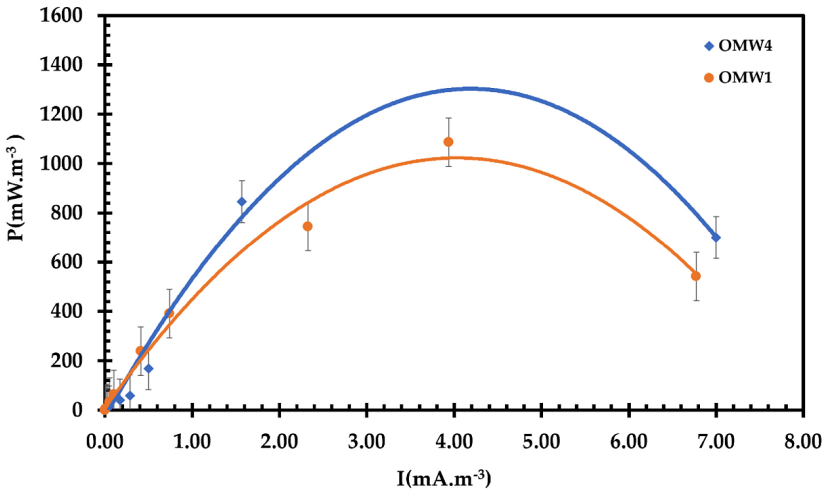


**Figure 4.** Power density curve of the MFC operated with the OMW sample

utilized an upflow MFC with halophilic consortium for the treatment of saline OMW. The maximum power density obtained was 439 mW.m$^{-2}$ at an optimized organic load of 1.52 g COD L$^{-1}$.

## Pollutants treatment effect with MFCs for two types of OMW

### *Phenolic compounds quantification and HPLC results*

The quantification and identification of phenolic compounds were carried out before and after MFC treatment. Figure 5 illustrates the initial and final concentrations, along with their corresponding removal rates, for samples OMW1 and OMW4. After five days of operation, the phenolic concentration in sample OMW1 decreased from 1 g L$^{-1}$ to 0.439 g L$^{-1}$, corresponding to a removal rate of 56.2%. In OMW4, a higher degradation efficiency of approximately 70.4% was achieved, with the concentration decreasing from 4 g L$^{-1}$ to 1.186 g L$^{-1}$. These results were confirmed by the polarization curves and power densities presented in Figures 3 and 4. The electrochemical performance observed is consistent with the degradation trends, affirming that higher removal rates are correlated with improved energy production in the MFC system.

High-performance liquid chromatography coupled with UV detection (HPLC-UV) was performed to evaluate the degradation profiles of phenolic compounds during MFC treatment. Tables 2 and 3 show the identified compounds in the two OMW samples. The standard mixture chromatogram was used to determine the separation of all identified compounds, with retention times (Rt) ranging from 5 to 17 min. According to this reference, five compounds were identified in the sample chromatogram. These are, in order of elution: (1) hydroxytyrosol (Rt ≈ 5.25 min; 13 mAU), (2) a second hydroxytyrosol peak (Rt ≈ 5.5 min; 19 mAU), (3) tyrosol (Rt ≈ 6.5 min; 5 mAU), (4) p-hydroxybenzoic acid (Rt ≈ 7.5 min; 4 mAU), and (5) luteolin-7-glucoside (Rt ≈ 9.25 min; 5 mAU). The most significant peak in this group is the second hydroxytyrosol peak at 19 mAU. Comparative analysis indicates that this compound was the most decomposed, as demonstrated by the maximum reduction in absorbance between the pre- and post-treatment chromatograms (Tekaya et al., 2022).

In Table 2, a total of nine compounds were identified from the sample chromatogram, in order of elution: (1) hydroxytyrosol (Rt ≈ 5.25 min; 70 mAU), (2) a second peak of hydroxytyrosol (Rt ≈ 5.5 min; 120 mAU), (3) tyrosol (Rt ≈ 6 min; 60 mAU), (4) a later peak of tyrosol (Rt ≈ 7 min; 400 mAU), (5) p-hydroxybenzoic acid (Rt ≈ 7.25 min; 40 mAU), (6) verbascoside (Rt ≈ 8.5 min; 60 mAU), (7–8) a doublet corresponding to luteolin-7-glucoside (Rt ≈ 9 min; 50 mAU), and (9) oleuropein (Rt ≈ 12 min). The highest peak in the chromatogram is the tyrosol peak at 400 mAU. This also revealed maximum degradation of this compound during treatment, as indicated by the greatest drop in absorbance between the pre- and post-treatment samples (Tekaya et al., 2022).

The MFC began by producing a specialized biofilm on its anode surface after OMW inoculation and system activation. The microbial community consists of toxic-tolerant microorganisms. The first step in breaking down complex phenolic compounds (hydroxytyrosol and oleuropein) involves enzymatic hydrolysis reactions. The

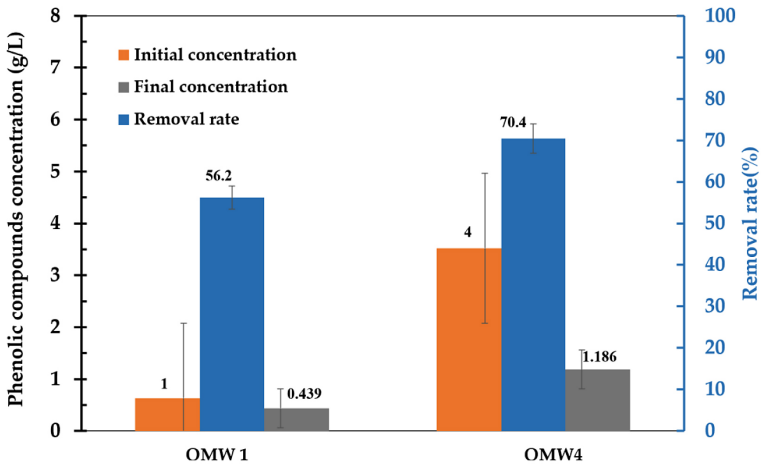


**Figure 5.** Evolution of phenolic concentrations in OMW1 and OMW4

**Table 2.** Identified phenolic compounds in OMW1 and their absorbance intensities using HPLC-UV analysis before and after MFC treatment

| Phenolic compound | Peak | Before treatment | | After treatment | | Absorbance decrease (%) | Total phenolic absorbances decrease (mAU) | Overall absorbance decrease (%) | Mean absorbance decrease (%) | Standard deviation (removal) |
|---|---|---|---|---|---|---|---|---|---|---|
| | | Absorbance (mAU) | Retention time (min) | Absorbance (mAU) | Retention time(min) | | | | | |
| Hydroxytyrosol | 1 | 13 | 5.25 | 10 | 5.25 | 23.08 | 23.5 | 36.09 | 43.33 | ± 15.40 |
| Hydroxytyrosol | 2 | 19 | 5.5 | 13 | 5.5 | 31.58 | | | | |
| Tyrosol | 3 | 5 | 6.5 | 2.2 | 6.5 | 56 | | | | |
| Hydroxybenzoic acid | 4 | 4 | 7.5 | 2 | 7.5 | 50 | | | | |
| Luteolin-7 glucoside | 5 | 5 | 9.25 | 2.2 | 9.25 | 56 | | | | |

**Table 3**. Identified phenolic compounds in OMW4 and their absorbance intensities using HPLC-UV analysis before and after MFC treatment

| Phenolic compound | Peak | Before treatment | | After treatment | | Absorbance decrease (%) | Total phenolic absorbances decrease (mAU) | Overall absorbance decrease (%) | Mean absorbance decrease (%) | Standard deviation (removal) |
|---|---|---|---|---|---|---|---|---|---|---|
| | | Absorbance before treatment (mAU) | Retention time (min) | Absorbance after treatment (mAU) | Retention time (min) | | | | | |
| Hydroxytyrosol | 1 | 70 | 5.25 | 40 | 5.25 | 42.86 | 502 | 61.6 | 51.2 ± 30.1% | ± 29.84 |
| Hydroxytyrosol | 2 | 120 | 5.5 | 75 | 5.5 | 37.50 | | | | |
| Tyrosol | 3 | 60 | 6 | 40 | 6 | 33.33 | | | | |
| Tyrosol | 4 | 400 | 7 | 70 | 7 | 82.50 | | | | |
| p-hydroxy-benzoic acid | 5 | 40 | 7.25 | 38 | 7.25 | 5 | | | | |
| Verbascoside | 6 | 60 | 8.5 | 25 | 8.5 | 58.33 | | | | |
| luteolin-7-glucoside | 7,8 | 50 | 9 | 25 | 9 | 50 | | | | |
| Oleuropein | 9 | 15 | 12 | – | 12 | 100 | | | | |

microbial community produces extracellular enzymes, including polyphenol oxidases (laccases and tyrosinases) and peroxidases. These enzymes break down large phenolic polymers into smaller aromatic monomers (catechol, gallic acid, and protocatechuic acid), which bacteria can readily consume.Bacterial cells of exoelectrogens use the simplified phenolic monomers as their carbon and energy sources, directing them into central metabolic pathways such as the β-ketoadipate pathway for catechol and protocatechuate degradation. The aromatic rings undergo intracellular enzymatic cleavage to produce succinyl-CoA and acetyl-CoA, which then enter the tricarboxylic acid (TCA) cycle. The respiratory chain of exoelectrogens produces electrons through NADH and $FADH_2$ oxidation during the breakdown of phenolic derivatives. The bacteria redirect these electrons away from natural terminal electron acceptors such as oxygen toward the insoluble anode. The complete breakdown of phenolic compounds results in the production of carbon dioxide and water while generating an electrical current. The external circuit enables electrons to move from the anode to the cathode, where they react with oxygen and protons from the anode chamber to form water. The anode reaction for a generic phenolic compound ($CH_2O$) produces the following overall reaction:

$$CH_2O \text{ (phenolic derivative)} + \\ + H_2O \rightarrow CO_2 + 4H^+ + 4 \quad (3)$$

### *COD measurements*

Figure 6 illustrates the COD removal rate in relation to phenolic concentrations, measured both at the start and after 5 days of operation. This duration was adopted to assess system stability under realistic operating conditions. The MFC system demonstrated substantial COD reduction rates exceeding 50%. Specifically, the MFC containing OMW1 achieved a removal rate of 52%. Notably, the MFC loaded with OMW4 delivered

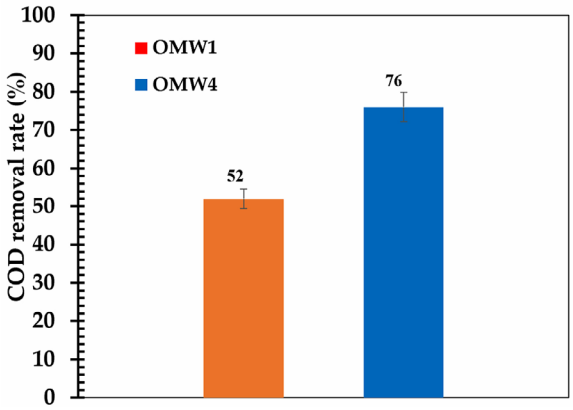


**Figure 6.** COD removal rate in the two samples after MFC treatment

the highest COD removal rate at 76%.These results align with the observed peak power outputs, as MFCs with greater organic matter degradation also generated more electricity. This is attributed to the increased availability of electrons produced at the anode, which are subsequently captured by the cathode and utilized in the oxygen reduction reaction (ORR), thereby enhancing both power generation and COD removal efficiency.

MFCs achieved a power density of up to 1200 $mW.m^{-3}$ with significant pollutant removal, indicating a compelling contrast with conventional electrochemical methods. More recent works concerning processes such as electro-Fenton (EF) have proven highly efficient in degrading recalcitrant organics in OMW. Despite the advantages of lower sludge generation compared to the Fenton process and high efficiency in removing a wide range of contaminants, this technique requires elevated operational costs (Soltani et al., 2022).A hybrid process investigated by De Carluccio et al. (2024) achieved higher purification results at the cost of energy input. Indeed, this work reported higher removal rates: COD and total phenolic compounds were removed at rates of 80–90% and 85–95%, respectively. However, it required significant energy consumption for the EF pre-treatment, which was necessary to detoxify the OMW and thus make it suitable for the subsequent biological stage. In contrast, the MFC system is a net energy-producing technology. The MFC concept—as pursued in our research—frames OMW as an energy resource while achieving robust COD removal of 52–76%, thus simultaneously treating it and offsetting operational costs through bioelectricity generation, offering a more sustainable economic model for decentralized application.In another study (Brillas et al., 2025) using EF with boron-doped diamond (BDD) anodes, almost complete OMW mineralization was reached, while COD and polyphenol removal rates exceeded 90%. Energy consumption for the treatment of high-organic-load wastewaters, including OMW, was reported to be on the order of tens to hundreds of $kWh \cdot m^{-3}$ – a value much higher than the energy output of the MFC. In a study by Jamrah et al. (2025), a coupled electrocoagulation-assisted adsorption (ECA) process yielded a final effluent quality illustrated by 72.88% COD removal, but it functioned as a net energy consumer with a significantly high operating cost of 14.31 $kWh.m^{-3}$ (USD 3.92.$m^{-3}$). In sharp contrast, the MFC system resulted in a comparable upper-range COD removal of 76% and a 70% reduction in phenolic compounds, while uniquely functioning as a net energy producer, generating 1028–1200 $mW.m^{-3}$ of bioelectricity.

## Coulombic efficiency determination

Table 4 represents parameters utilized in the calculation of this efficiency, after OMW1 and OMW4 treatment (Chen et al., 2021).

**Table 4.** Parameters (COD removed, current density range and operating time) included in OMWs treatment

| Parameter | OMW1 | OMW4 |
|---|---|---|
| Electrode volume ($m^3$) | $1.25 \times 10^{-4}$ | $1.25 \times 10^{-4}$ |
| Initial COD (mg $L^{-1}$) | 22 550 | 43 750 |
| COD removal rate (%) | 52 | 76 |
| ΔCOD (mg $L^{-1}$) | 11 726 | 32 812.5 |
| ΔCOD (kg.$m^{-3}$) | 11.726 | 32.8125 |
| Current density range (mA.$m^{-3}$) | 0 – 8 | 0 – 8 |
| Operating time (s) | 432 000 (5 days) | 432 000 (5 days) |

**For OMW1:**

$$\Delta S = \frac{\Delta COD}{M(O_2)} = \frac{11.726\ (g\ L^{-1})}{32\ (g\ mol^{-1})} = 0.36644\ mol\ O_2\ L^{-1}$$

$$\Delta S\ (per\ m^3) = 0.36644 \times 1000$$

$$= 366.44\ mol\ O_2\ m^{-3}$$

Theoretical total charge from substrate:

$$Q_{th} = F \times b \times V_{an} \times \Delta S\ (mol \cdot m^{-3})$$

$$Q_{th} = 96{,}485 \times 4 \times (1.25 \times 10^{-4}) \times 366.44 = 17{,}681\ C$$

Medium $U_{cell} \approx 0.3155$ V.

$$P = \frac{U_{cell} \cdot I_{cell}}{V_{an}}$$

$$I_{cell} = \frac{P.V_{an}}{U_{cell}}$$

$$I_{cell} = \frac{1.028\ (W.m^{-3}) \times 1.25\times10^{-4}\ (m^3)}{0.3155\ (V)} = \frac{1.285.\times10^{-4}}{0.3155}$$

$$I_{cell} = 4.073\times10^{-4}\ (A) = 0.4073\ (mA)$$

$$Q_{actual} = I_{cell} \times t = 4.073\times10^{-4}\ (A)\times 432\ 000\ (s)$$

$$Q_{actual} = 175.95\ C$$

$$CE = \frac{Qactual}{Qth}\times 100\ (\%) = \frac{175.95}{17\ 681} \approx 1\%$$

**For OMW4 :**

$$\Delta S = \frac{\Delta COD}{M(O_2)} = \frac{32.8125\ (g\ L^{-1})}{32\ (g\ mol^{-1})} = 1.02539\ mol\ O_2\ L^{-1}$$

$$= 1025.39\ mol\ O_2 \cdot m^{-3}$$

$$Q_{th} = 96485\times4\times(1.25\times10^{-4})\times1025.39$$

$$Q_{th} = 48.2425\times1025.39 \approx 49470\ C$$

Medium $U_{cell} \approx 0.3$ V.

$$I_{cell} = \frac{1.2\ (W.m^{-3}) \times 1.25\times10^{-4}(m^3)}{0.3\ (V)} = 0.0005$$

$$A = 0.5\ mA$$

$$Q_{actual} = 0.0005\times432\ 000 = 216\ C$$

$$CE = \frac{216}{49\ 470} \times 100\% \approx 0.436\%$$

The CE values reported for OMW1 (1%) and OMW4 (0.436%) clearly show that only a small percentage of the removed organic matter was converted into electric current, while the majority of substrate oxidation occured via non-electrogenic routes such as fermentation. The slightly higher CE value reported for OMW1 compared to OMW4 may be due to the lower phenolic and COD concentrations in OMW1 (1 g $L^{-1}$ and 22.55 g $L^{-1}$, respectively), resulting in a less inhibitory environment for exoelectrogenic bacteria. This may have resulted in slightly greater electron transfer to the anode. On the other hand, the substantially lower CE reported for OMW4 (0.436%) compared to OMW1, despite having a greater COD removal (76%) and phenolic removal (70.4%) rates, may be due to the high substrate richness in OMW4 (4 g $L^{-1}$ phenols and 43.75 g $L^{-1}$ COD). It may have favored the development of competitive non-electrogenic bacteria, outcompeting exoelectrogenic bacteria for the available organic substrate. These findings align with previous studies on complex OMWs, where high substrate concentrations and phenolic inhibition are known to suppress exoelectrogenic activity, resulting in CE values normally below 5% (Raychaudhuri and Behera, 2023; Pugazhendi and Jamal, 2023). However, while these results may not be ideal for MFC operation as a bioelectrochemical reactor for electricity generation, they do highlight the overall efficiency of the MFC as a bioremediation technology for OMW treatment, as evidenced by the high COD and phenolic removal rates observed.

### *Heavy metals removal*

Table 5 presents the initial concentrations and removal efficiencies of heavy metals in two types of OMW, identified as OMW1 and OMW4. Initially, Ni and Mg exist in relatively high quantities, especially in OMW4 (Ni:10.07 mg $L^{-1}$; Mg: 24.78 mg $L^{-1}$), while Co and Cr are found in very low concentrations. Cu and Fe are also well represented, with higher amounts of Cu in OMW1 and higher levels of Fe in OMW4.

After treatment, Cr was completely removed (100%) in OMW1, and Co achieved full removal in both OMW1 and OMW4, indicating a strong

**Table 5.** Removal rates of heavy metals

| Metal species | Initial concentrations in OMW (mg $L^{-1}$) | | Removal rates of heavy metals (%) | |
|---|---|---|---|---|
| | OMW1 | OMW4 | OMW1 | OMW4 |
| Cr | 0.14 | 0.09 | 100 | 52.66 |
| Zn | 1.5408 | 1.8904 | 88.84 | 85.11 |
| Cd | 0.2805 | 0.459 | 49.76 | 43.63 |
| Ni | 6.0196 | 10.0722 | 42.32 | 30.29 |
| Co | 0.0633 | 0.0119 | 100 | 100 |
| Fe | 2.7418 | 5.8071 | 13.37 | 5.18 |
| Mg | 21.8755 | 24.7806 | 6.59 | 5.25 |
| Cu | 11.2553 | 8.2791 | 71.44 | 97.40 |

affinity between the system and these specific metals. Cu exhibited excellent removal performance, particularly in OMW4 (97.40%). Zn also showed consistently high removal efficiencies in both samples (>85%), highlighting its favorable response to the treatment process. Conversely, Fe, Mg, Ni, and Cd displayed comparatively lower removal rates, especially in OMW4. These reduced efficiencies may be linked to factors such as chemical speciation and solubility. In summary, the treatment system appears to be more effective with OMW1 for most metals, particularly Cr, Cu, Ni, and Fe.

The high removal rate observed for heavy metals in this system suggests that biosorption may be the primary mechanism involved. This process relies on microbial biomass, known as biosorbents, which interact with metals through physicochemical forces such as complexation and microprecipitation. These interactions are facilitated by the cellular wall components of bacteria, which contain polysaccharides, proteins, and lipids bearing carboxylate, hydroxyl, phosphate, amine, and sulfate functional groups (Vullo et al., 2008). Additionally, the membrane used in this study contains an ionic liquid—specifically methyltrioctyl ammonium chloride—which has also played a role in the removal of metal ions through adsorption, as previously documented (De Los Ríos et al., 2012).

## Kinetic modeling and energy analysis

The kinetic modelling can be divided into three components, regarding phenolic compounds, COD degradation and power density.

### *Phenolic compounds degradation kinetics*

The reduction in phenolic concentration follows a first-order reaction rate, assuming the microbial community's activity is the limiting factor (Akatah and Bariture, 2023).

General equation:

$$\frac{dC}{dt} = -k_{Ph} \times C$$

Integrated form:

$$\ln\left(\frac{C_0}{C_t}\right) = k_{Ph} \times t$$

where: $C_0$ – initial phenolic concentration (g $L^{-1}$), $C_t$ – final phenolic concentration after time t (g $L^{-1}$), $k_{Ph}$ – phenolic degradation rate constant ($day^{-1}$), t = time (days).

**For OMW1:**

$$C_0 = 1\ ,\ C_t = 0.438,\ t = 5 \text{ days}$$

$$k_{Ph1} = \frac{\ln\left(\frac{1}{0.438}\right)}{5} = \frac{\ln(2.283)}{5} = 0.165 \text{ day}^{-1}$$

**For OMW4:**

$$C_0 = 4\ ,\ C_t = 1.186,\ t = 5 \text{ days}$$

$$k_{Ph4} = \frac{\ln\left(\frac{4}{1.186}\right)}{5} = \frac{\ln(3.373)}{5} = 0.243 \text{ day}^{-1}$$

The half-life ($t_{1/2}$) of a first-order reaction does not depend on the initial concentration of the substrate and can be calculated by the following equation:

$$t_{1/2} = \frac{\ln(2)}{k_{Ph}}$$

The kinetic results indicate that phenolic degradation for both OMW samples follows a first-order kinetic pattern, with OMW4 showing a significantly higher rate constant for phenolic degradation ($k_{Ph4}$ = 0.243 $day^{-1}$) than OMW1 ($k_{Ph1}$ = 0.165 $day^{-1}$), i.e., a 47.3% enhancement in rate constant, despite a four times higher initial phenolic concentration for OMW4 (4 g $L^{-1}$) than OMW1(1 g $L^{-1}$). This is a non-intuitive result, implying that instead of exerting inhibitory effects, the higher organic matrix content in OMW4 probably stimulated higher acclimation rates, electroactive biofilm formation, and synergistic co-metabolic degradation pathways, all of which contributed to a faster phenolic degradation rate. The better kinetic performance of OMW4 is further supported by a faster half-life time for OMW4 ($t_{1/2}$ = 2.85 days) than OMW1 ($t_{1/2}$ = 4.20 days), which confirms that a higher substrate concentration is less inhibitory to phenolic degradation when a well-acclimated biofilm is present. Accordingly, these results confirm that the MFC system performs better under higher substrate concentrations, while the improved kinetic performance for OMW4 supports the conclusion that a higher substrate concentration has a positive influence on bioelectrochemical phenolic degradation.

### *COD removal kinetics*

Similarly, COD removal is modeled using first-order kinetics,following the equation below (Akatah and Bariture, 2023):

$$\ln\left(\frac{COD_0}{COD_t}\right) = k_{COD} \times t$$

**Table 6.** Energy input components

| Component | OMW1 | OMW4 | Notes |
|---|---|---|---|
| Pumping energy (kWh.m$^{-3}$) | 0.15 | 0.15 | Assumed for recirculation |
| Aeration energy (kWh.m$^{-3}$) | 0 | 0 | MFC operates anaerobically |
| Temperature control (kWh.m$^{-3}$) | 0 | 0 | Ambient operation (25°C) |
| Monitoring & control (kWh.m$^{-3}$) | 0.05 | 0.05 | Instrumentation |
| Total energy input (kWh.m$^{-3}$) | 0.20 | 0.20 | Constant across both samples |

The removal rates (52% for OMW1, 76% for OMW4) are used to determine $k_{COD}$ assuming

$$COD_t = COD_0 \times (1 - \text{removal rate}).$$

**For OMW1:**

$$\text{The removal rate is } 52\% \rightarrow \frac{COD_t}{COD_0} = 0.48$$

$$k_{COD1} = \frac{\ln\left(\frac{1}{0.48}\right)}{5} = \frac{\ln(2.083)}{5} = 0.147 \text{ day}^{-1}$$

**For OMW4:**

$$\text{The removal rate is } 76\% \rightarrow \frac{COD_t}{COD_0} = 0.24$$

$$k_{COD4} = \frac{\ln\left(\frac{1}{0.24}\right)}{5} = \frac{1.4271}{5} = 0.285 \text{ day}^{-1}$$

The kinetic analysis of COD degradation for OMW4 shows that there was a significant improvement in the first-order rate constant for COD degradation ($k_{COD4}$= 0.285 day$^{-1}$) compared to OMW1 ($k_{COD1}$= 0.147 day$^{-1}$). There was a 93.9% improvement in the rate constant for OMW4, despite having a higher organic load. This significant improvement in COD degradation kinetics for OMW4 was consistent with the higher efficiency of COD removal for OMW4 (76%) compared to OMW1 (52%). The half-life for COD degradation was significantly lower for OMW4 (2.43 days) than for OMW1 (4.72 days). This shows that higher organic loading to the MFC system was conducive to faster organic matter degradation. A higher rate constant for COD degradation was also obtained for OMW4 (0.285 day$^{-1}$) than for phenolic degradation (0.243 day$^{-1}$). This shows that the microbial population in the MFC system was more efficient at degrading organic matter in OMW4, which was a complex organic matter containing non-phenolic biodegradable organic compounds.

*Energy balance comparison*

For a comprehensive energy balance, the following energy components are considered:

a) Energy input analysis – Table 6 represents the different components for energy input analysis.

b) Energy output analysis – the electrical energy generated by the MFC is calculated as:

$$E_{elec} = P \times t \times V_{reactor}$$

where: P – power density (mW.m$^{-3}$), t – operating time (days), $V_{reactor}$ – reactor volume (assumed 1 m$^3$ for normalization).

**For OMW1**: $E_{elec}$ =1028 (mW.m$^{-3}$) ×120 (h)/1000 = 0.1233 kWh.m$^{-3}$

**For OMW 4:** $E_{elec}$ =1200 (mW.m$^{-3}$)×120 (h)/1000 = 0.144 kWh.m$^{-3}$

c) Chemical energy recovered (COD removal) – the chemical energy equivalent of removed COD represents the energy value of the organic matter that was degraded (Jafary et al., 2026):

$$E_{chem} = \Delta_{COD} \times \Delta H_{COD}$$

where: $\Delta_{COD}$ – COD removed (kg.m$^{-3}$), $\Delta H_{COD}$ – energy equivalent of COD (3.86 kWh.kg$^{-1}$ COD).

**Table 7.** Electrical energy output

| Parameter | OMW1 | OMW4 |
|---|---|---|
| Max power density (mW·m$^{-3}$) | 1028 | 1200 |
| Operating time (days) | 5 | 5 |
| Operating time (hours) | 120 | 120 |
| Electrical energy output (kWh·m$^{-3}$) | 0.1233 | 0.144 |

**Table 8**. Chemical energy recovery

| Parameter | OMW1 | OMW4 |
|---|---|---|
| Initial COD (kg.m$^{-3}$) | 50.0* | 200.0* |
| Final COD (kg.m$^{-3}$) | 24.2 | 50.9 |
| COD removed (kg.m$^{-3}$) | 25.8 | 149.1 |
| COD removal efficiency (%) | 51.6 | 74.55 |
| Chemical energy equivalent (kWh.m$^{-3}$) | 99.6 | 575.5 |

**Note:** * Estimated, based on typical OMW characteristics and phenolic/COD ratios.

**Table 9**. Total energy output summary

| Component | OMW1 | OMW4 |
|---|---|---|
| Electrical energy (kWh.m$^{-3}$) | 0.1233 | 0.144 |
| Chemical energy (COD removed) (kWh.m$^{-3}$) | 99.6 | 575.5 |
| Total energy output (kWh.m$^{-3}$) | 99.7233 | 575.644 |

**Table 10**. Complete energy balance

| Parameter | OMW1 | OMW4 |
|---|---|---|
| Energy input (kWh.m$^{-3}$) | 0.20 | 0.20 |
| Energy output (kWh.m$^{-3}$) | 99.72 | 575.64 |
| Net energy gain (kWh.m$^{-3}$) | +99.52 | +575.14 |

**Table 11**. Net energy results

| Parameter | OMW1 | OMW4 |
|---|---|---|
| Total energy output (kWh.m$^{-3}$) | 99.72 | 575.64 |
| Total energy input (kWh.m$^{-3}$) | 0.20 | 0.20 |
| Net energy (kWh.m$^{-3}$) | +99.52 | +575.14 |
| Net electrical energy (kWh.m$^{-3}$) | -0.0767 | -0.056 |

$$E_{net,elec,OMW1} = 0.1233 - 0.20 = -0.0767\ kWh \cdot m^{-3}$$

$$E_{net,elec,OMW4} = 0.144 - 0.20 = -0.056\ kWh \cdot m^{-3}$$

$$E_{chem,OMW1} = 25.8\ (kg \cdot m^{-3}) \times 3.86\ (kW \cdot kg^{-1}) = 99.6\ kWh \cdot m^{-3}$$

$$E_{chem,OMW4} = 149.1\ (kg \cdot m^{-3}) \times 3.86\ (kWh \cdot kg^{-1}) = 575.5\ kWh \cdot m^{-3}$$

d) Total energy output

$$E_{total,out} = E_{elec} + E_{chem}$$

Energy balance can be summarized in Table 10, where energy input, output, and net energy gain are presented.

### *Determination of net energy*

Net energy represents the difference between total energy recovered and total energy consumed:

$$E_{net} = E_{total,out} - E_{in}$$

From the energy balance analysis, it is apparent that there is a stark contrast in terms of the electrical and chemical energy recovered from the two OMW samples. Although the amount of electrical energy recovered from both MFCs was still relatively low for OMW1 (0.1233 kWh·m$^{-3}$) and OMW4 (0.144 kWh·m$^{-3}$), the chemical energy equivalent of the COD removal was considerably higher at 99.6 kWh·m$^{-3}$ for OMW1 and 575.5 kWh·m$^{-3}$ for OMW4. As a result, the total energy output was dominated by the chemical energy component, rendering the electrical component negligible (<0.15% for both MFCs). As the energy input for the pumping and monitoring of the MFCs was kept constant at 0.20 kWh·m$^{-3}$, it is apparent that the net energy output was highly positive for both MFCs at +99.52 kWh·m$^{-3}$ and +575.14 kWh·m$^{-3}$ for OMW1 and OMW4. In terms of the actual electrical energy recovered from both MFCs, it is apparent that both MFCs would still suffer from a net loss in terms of electrical energy harvested from the wastewater, at -0.0767 kWh·m$^{-3}$ for OMW1 and -0.056 kWh·m$^{-3}$ for OMW4. This clearly demonstrates that the MFC is an energetically favorable technology for the treatment of OMW, in which the chemical energy recovered from the COD removal is considerably higher than the actual energy input for the pumping and monitoring of the MFC.

## CONCLUSIONS

This study explored the impact of phenolic compound concentration on bioelectricity production, COD reduction, and heavy metal removal from olive mill wastewater at the laboratory scale. The main outcomes can be summarized as follows:

1. Bioelectrogenic performance improved markedly under higher phenolic loads, demonstrating that these compounds can act as a valuable carbon source for electricity generation.
2. The maximum power density increased from 1028 mW·m$^{-3}$ for OMW1 (1 g·L$^{-1}$ phenolics) to 1200 mW·m$^{-3}$ for OMW4 (4 g·L$^{-1}$ phenolics), highlighting the strong influence of substrate composition on MFC efficiency.
3. Phenolic compounds and COD were effectively degraded, with maximum removal rates of 70.4% and 76%, respectively, for the OMW4 sample.
4. Heavy metals were also efficiently removed, with rates ranging from 30% to 97% across all species analyzed.
5. Even with an increased phenolic content by a factor of four (4 g·L$^{-1}$ against 1 g·L$^{-1}$), OMW4 displayed an elevated first-order rate constant for phenolic removal (0.243 day$^{-1}$) by 47.3% and for COD removal (0.285 day$^{-1}$) by 93.9% in comparison to OMW1. This suggests that greater organic loads facilitated biofilm adaptation, exoelectrogenesis, and co-metabolism than inhibition.

6. At an equal energy input of 0.20 kWh·m$^{-3}$, both scenarios yielded high net energy gains (+99.52 and +575.14 kWh·m$^{-3}$), but net electrical energy was still negative (−0.0767 and −0.056 kWh·m$^{-3}$). This highlights that the MFC is more useful in wastewater treatment through positive energy utilization than as a source of sustainable electrical energy.

These results highlight the potential of MFCs to turn OMW into bioelectricity while detoxifying the effluent, offering a sustainable platform for future optimization and scale-up toward circular energy solutions.

## REFERENCES


1. Abubakar, I.R., Maniruzzaman, K.M., Dano, U.L., Al Shihri, F.S., Al Shammari, M.S., Ahmed, S.M.S., Al-Gehlani, W.A.G, Alrawaf T.I. (2022). Environmental sustainability impacts of solid waste management practices in the Global South. *Int. J. Environ. Res. Public Health*, *19*, 12717. https://doi.org/10.3390/ijerph191912717.
2. Agabo-García, C., Repetto, G., Albqmi, M., Hodaifa, G. (2023). Evaluation of the olive mill wastewater treatment based on advanced oxidation processes (AOPs), flocculation, and filtration. *Journal of Environmental Chemical Engineering*, *11*, 109789. https://doi.org/10.1016/j.jece.2023.109789.
3. Ahmed, H.R., Ealias, A.M., George, G. (2025). Advanced oxidation processes for the removal of antidepressants from wastewater: A comprehensive review. *RSC Adv*, *15*, 48639–48665. https://doi.org/10.1039/D5RA07764H.
4. Akatah, B.M., Bariture, L.C. (2023). Comparative study of the first order kinetics and fractal kinetics of substrate utilization from septic wastewater in a packed bed microbial fuel cell (MFC). *International Journal of Engineering Science and Computing*, *13*.
5. Antonopoulou, G., Bampos, G., Ntaikou, I., Alexandropoulou, M., Dailianis, S., Bebelis, S., Lyberatos, G. (2023). The biochemical and electrochemical characteristics of a microbial fuel cell used to produce electricity from olive mill wastewater. *Energy*, *282*, 128804. https://doi.org/10.1016/j.energy.2023.128804.
6. Athanasiadis, V., Voulgaris, A., Katsoulis, K., Lalas, S.I., Roussis, I.G., Gortzi, O. (2023). Development of enriched oil with polyphenols extracted from olive mill wastewater. *Foods*, 12. https://doi.org/10.3390/foods12030497.
7. Awasthi, M.K., Paul, A., Kumar, V., Sar, T., Kumar, D., Sarsaiya, S., Liu, H., Zhang, Z., Binod, P., Sindhu, R. (2022). Recent trends and developments on integrated biochemical conversion process for valorization of dairy waste to value added bioproducts: A review. *Bioresource Technology,344*, 126193. https://doi.org/10.1016/j.biortech.2021.126193.
8. Benzaouak, A., Touach, N., Ortiz-Martínez, V.M., Salar-García, M.J., Hernández-Fernández, F., De Los Ríos, A.P., El Mahi, M., Lotfi, E.M. (2018). Ferroelectric solid solution Li1− xTa1− xWxO3 as potential photocatalysts in microbial fuel cells: Effect of the W content. *Chinese Journal of Chemical Engineering, 26*(9), 1985–1991. https://doi.org/10.1016/j.cjche.2018.02.008.
9. Bouigua, H., Bakali, R., Jaber, H., El Kabous, K., Choukri, S., Elyachioui, M., Ouhssine, M. (2024). A remarkable step in the aerobic biological treatment of olive mill wastewater (OMW): A combination of selected microbial strains that enhance their decolorization and depollution. *E3S Web Conf. 527*, The 4th Edition of Oriental Days for the Environment "Green Lab. Solution for Sustainable Development" (JOE4). https://doi.org/10.1051/e3sconf/202452702007.
10. Brillas, E., Garcia-Segura, S. (2025). Electrochemical advanced oxidation processes for real wastewater remediation: Systems, performance, and generated oxidants. *ACS Electrochemistry, 1*, 2292–2316. https://doi.org/10.1021/acselectrochem.5c00311.
11. Chen,W., Huang, Y.X., Li, D.B., Yu, H.Q., Yan, L. (2014). Preparation of a macroporous flexible three dimensional graphene sponge using an ice-template as the anode material for microbial fuel cells. *RSC Adv*., *4*(41), 21619–21624. https://doi.org/10.1039/C4RA00914B.
12. Chen, W., Liu, Z., Li, Y., Xing, X., Liao, Q., & Zhu, X. (2021). Improved electricity generation, coulombic efficiency and microbial community structure of microbial fuel cells using sodium citrate as an effective additive. *Journal of Power Sources*, *482*, 228947. https://doi.org/10.1016/j.jpowsour.2020.228947.
13. Choe, C., Cheon, S., Gu,J., Lim, H. (2022). Critical aspect of renewable syngas production for power-to-fuel via solid oxide electrolysis: Integrative assessment for potential renewable energy source. *Renewable and Sustainable Energy Reviews,161*, 112398. https://doi.org/10.1016/j.rser.2022.112398.
14. Choudhury, P., Bhunia, B., Mahata, N., Bandyopadhyay, T.K. (2022). Optimization for the improvement of power in equal volume of single chamber microbial fuel cell using dairy wastewater. *Journal of the Indian Chemical Society, 99*, 100489. https://doi.org/10.1016/j.jics.2022.100489.
15. De Carluccio, M., Barboza, P., Attarian, P., Ahangarnokolaei, M.A., Rizzo, L. (2024). Olive mill wastewater co-treatment: Effect of (electro)Fenton processes and dilution ratio on moving bed biofilm reactor performance. *Journal of Cleaner Production, 447*, 141526. https://doi.org/10.1016/j.jclepro.2024.141526.

16. De Los Ríos, A.P., Hernández-Fernández, F.J., Alguacil, F.J., Lozano, L.J., Ginestá, A., García-Díaz, I., Sánchez-Segado, S., López, F.A., Godínez, C. (2012). On the use of imidazolium and ammonium-based ionic liquids as green solvents for the selective recovery of Zn(II), Cd(II), Cu(II) and Fe(III) from hydrochloride aqueous solutions. *Separation and Purification Technology, 97*,150–157. https://doi.org/10.1016/j.seppur.2012.02.040.
17. De Souza Melaré,V.A.,Montenegro González, S., Faceli, K., Casadei, V. (2017). Technologies and decision support systems to aid solid-waste management: A systematic review. *Waste Management, 59*, 567–584. https://doi.org/10.1016/j.wasman.2016.10.045.
18. Dich, A., Abdelmoumene, W., Belyagoubi, L., Assadpour, E., Belyagoubi Benhammou, N., Zhang, F., Jafari., S.M. (2025). Olive oil wastewater: a comprehensive review on examination of toxicity, valorization strategies, composition, and modern management approaches. *Environmental Science and Pollution Research*, *32*, 6349–6379.
19. Djeziri, S.,Taleb, Z., Djellouli, H.M., Taleb,S. (2023). Physicochemical and microbiological characterisation of olive oil mill wastewater (OMW) from the region of Sidi Bel Abbes (western Algeria). *Moroccan Journal of Chemistry*, *11*, 506–20. https://doi.org/10.48317/IMIST.PRSM/morjchem-v11i2.31935.
20. Ferronato, N., Torretta, V .(2019). Waste mismanagement in developing countries: A review of Global issues. *International Journal of Environmental Research and Public Healt*h, 16, 1060. https://doi.org/10.3390/ijerph16061060.
21. Gucbilmez, Y. (2022). Physiochemical properties and removal methods of phenolic compounds from waste waters. Persistent organic pollutants (POPs) – monitoring, impact and treatment. https://doi.org/10.5772/intechopen.101545.
22. Gueboudji, Z., Kadi, K., Nagaz, K. (2021). Extraction and quantification of polyphenols of olive oil mill wastewater from the cold extraction of olive oil in the region of Khenchela, Algeria. *GSC Advanced Research and Reviews*, *5*, 116–22. https://doi.org/10.46325/gabj.v5i2.79.
23. Güneş, S., Ayol, A., Tezer, O. (2025). Biodegradation and power generation from olive oil mill wastewater using soil-based microbial fuel cells. *International Journal of Hydrogen Energy*, 116, 410-419. https://doi.org/10.1016/j.ijhydene.2025.03.081.
24. Hitar, M.E.H., Benzaouak, A., Touach, N., Kharti, H., Assani, A., El Mahi, M., Lotfi, E.M. (2024). Sustainable electricity generation using $LiTaO_3$-modified $Mn^{2+}$ ferroelectric photocathode in microbial fuel cells: Structural insights and enhanced waste bioconversion. *Chemical Physics Letters*, *837*, 141055. https://doi.org/10.1016/j.cplett.2023.141055.
25. Ishita, A., Dauksas, E., Remme, J.F., Richardsen, R., Kristin Løes, A. (2020). Fish and fish waste-based fertilizers in organic farming – with status in Norway: A review. *Waste Management*, *115*, 95–112. https://doi.org/10.1016/j.wasman.2020.07.025.
26. Jafary, T., Mousavi, A., Yeneneh, A.M., Saif Al-Kalbani, M., Al-Wahaibi, B.M. (2026). Recent advances in scaling up microbial fuel cell systems for wastewater treatment. *Energy Recovery, and Environmental Sustainability*, *18*, 638. https://doi.org/10.3390/su18020638.
27. Jamrah, A., Al-Zghoul, T.M., Al-Qodah, Z., Al-Karablieh, E. (2025). Performance of combined olive mills wastewater treatment system: Electrocoagulation-assisted adsorption as a post polishing sustainable process. *Water*, *17*, 1697. https://doi.org/10.3390/w17111697.
28. Jarboui, R., Magdich, S., Ammar, E. (2023). Open ponds for effluent storage, a pertinent issue to olive mill wastewater (OMW) management in a circular economy context: Benefits and environmental impact. Chapter 7. https://doi.org/10.1007/978-3-031-23449-1_7.
29. Kaza, S., Yao, L.C., Perinaz, B.T., Van Woerden, F. (2018). What a waste 2.0: A global snapshot of solid waste management to 2050. Urban Development, World Bank. https://doi.org/10.1596/978-1-4648-1329-0.
30. Khabirul Islam, A.K.M., Dunlop, P.S.M., Bhattacharya, G., Mkim, M., Hewitt, N.J., Huang, Y., Gogulancea, V., Zhang, K., Brandoni, C. (2023). Comparative performance of sustainable anode materials in microbial fuel cells (MFCs) for electricity generation from wastewater. *Results in Engineering*, *20*, 101385. https://doi.org/10.1016/j.rineng.2023.101385.
31. Kilemile, W., Vulla, K.E., Mihafu, F., Chandrasekaran, V. (2025). Transforming food systems: A Review of Sustainable Approaches to Minimize Food loss and waste. *Food Science & Nutrition*, *13*, 71167. https://doi.org/10.1002/fsn3.71167.
32. Larrosa-Guerrero, A., Scott, K., Mateo, F., Ginesta, A., Godinez, C. (2010). Effect of temperature on the performance of microbial fuel cells. *Fuel*, *89*, 3985-3994. https://doi.org/10.1016/j.fuel.2010.06.025.
33. Ma, J., Chen, D., Zhang, W., An, Z., Zeng, K., Yuan, M., Shen, J. (2021). Enhanced Performance and degradation of wastewater in microbial fuel cells using titanium dioxide nanowire photocathodes. *RSC Advances*, *11*, 2242–52. https://doi.org/10.1039/d0ra08747e.
34. Mannaf, M.M., Rahman, Md., M, Sabuj, S.T., Talukder, N., Lee, E.S. (2025). Current progress in advanced functional membranes for water-pollutant removal: A critical review. *Membranes* (Basel), *15*, 300. https://doi.org/10.3390/membranes15100300.

35. Palatsi, J.; Laureni, M.; Andrés, M.V.; Flotats, X.; Nielsen, H.B.; Angelidaki, I. (2009). Strategies for recovering inhibition caused by long chain fatty acids on anaerobic thermophilic biogas reactors. *Bioresource Technology*, *100*, 4588–4596. https://doi.org/10.1016/j.biortech.2009.04.046.

36. Pugazhendi, A., Jamal, M.T. (2023). Application of halophiles in UMFC (upflow microbial fuel cell) for the treatment of saline olive oil industrial wastewater coupled with eco-energy yield. *3 Biotech*, *13*, 351. https://doi.org/10.1007/s13205-023-03772-z.

37. Raychaudhuri, A., Behera, M. (2023). Biodegradation and power production kinetics in microbial fuel cell during rice mill wastewater treatment. *Fuel*, *339*, 126904. https://doi.org/10.1016/j.fuel.2022.126904.

38. Rehman, F.U., Amjad, F., Lee, W., Chang, M. (2025). Recent advances in functional energy materials for microbial fuel cells: progress, challenges, and future perspectives. *Journal of Materials Chemistry A*, *13*, 32056–32103. https://doi.org/10.1039/D5TA04072H.

39. Shah, A.M., Zhang, H., Shahid, M., Ghazal, H., Shah, A.R., Niaz, M., Naz, T., Ghimire, K., Goswami, N., Shi, W., Xia, D., Zhao, H. (2025). The vital roles of agricultural crop residues and agro-industrial by-products to support sustainable livestock productivity in subtropical regions. *Animals*, *15*, 1184. https://doi.org/10.3390/ani15081184.

40. Solomakou, N., Goula, A.M. (2021). Treatment of olive mill wastewater by adsorption of phenolic compounds. *Reviews in Environmental Science and Bio/Technology*, *20*, 839–863. https://doi.org/10.1007/s11157-021-09585-x.

41. Soltani, F., Navidjouy, N., Rahimnejad, M. (2022). A review on bio-electro-Fenton systems as environmentally friendly methods for degradation of environmental organic pollutants in wastewater. *RSC Advances*, *12*, 5184–5213. https://doi.org/10.1039/D1RA08825D.

42. Tekaya, M., Chehab, H., Guesmi, A., Algethami, F.K., Ben Hamadi, N., Hammami, M., Mechri, B. (2022). Study of phenolic composition of olive fruits: validation of a simple and fast HPLC-UV method. *OCL*, *29*. https://doi.org/10.1051/ocl/2022028.

43. Torres, C.I., Marcus, A.K., Lee, H.S., Parameswaran, P., Krajmalnik-Brown, R., Rittmann, B.E. (2010). A kinetic perspective on extracellular electron transfer by anode-respiring bacteria FEMS. *Microbiology Reviews*, *34*, 3–17, https://doi.org/10.1111/j.1574-6976.2009.00191.x.

44. Touach, N., Benzaouak, A., Toyir, J., Lotfi, E.M., Labjar, N., El Hamdouni, Y., El Mahi, M., Kacimi, M., Liotta, L.F. (2023). $BaTiO_3$ functional perovskite as photocathode in microbial fuel cells for energy production and wastewater treatment. *Molecules*, *28*, 1–13. https://doi.org/10.3390/molecules28041894.

45. Touach, N., Ortiz-Martínez, V.M., Salar-García, M.J., Benzaouak, A., Hernández-Fernández, F., De Los Ríos, A.P., El Mahi, M., Lotfi, E.M. (2017). On the use of ferroelectric material $LiNbO_3$ as novel photocatalyst in wastewater-fed microbial fuel cells. *Particuology*, *34*, 147–155. https://doi.org/10.1016/j.partic.2017.02.006.

46. Ucar, D., Zhang, Y., Angelidaki, I. (2017). An overview of electron acceptors in microbial fuel cells. *Frontiers in Microbiology*, *8*, 643. https://doi.org/10.3389/fmicb.2017.00643.

47. Vaz, T., Domingues, S., Martins, R.C., Gomes,J., Margarida, J. (2025). Quina ozonation to enhance methane production in anaerobic digestion of olive oil industry wastewater. *Journal of Environmental Chemical Engineering*, *13*, 117888 .https://doi.org/10.1016/j.jece.2025.117888 .

48. Vullo, D.L., Ceretti, H.M., Daniel, M.A., Ramirez, S.A.M., Zalts, A. (2008). Cadmium, zinc and copper biosorption mediated by *Pseudomonas veronii* 2E. *Bioresource Technology*, *99*, 5574–5581. https://doi.org/10.1016/j.biortech.2007.10.060.

49. Wainaina, S., Awasthi, M.K., Sarsaiya, S., Chen, H., Singh, E., Kumar, A., Ravindran, B., KumarAthi, S., Liu, T., Duan, Y., Kumar, S., Zhang, Z., Taherzadeh, M.J. (2020). Resource recovery and circular economy from organic solid waste using aerobic and anaerobic digestion technologies. *Bioresource Technology*, *301*, 122778. https://doi.org/10.1016/j.biortech.2020.122778.

50. Watson, V.J., Logan, B.E. (2011). Analysis of polarization methods for elimination of power overshoot in microbial fuel cells. *Electrochemistry Communications*, *13*, 54–56. https://doi.org/10.1016/j.elecom.2010.11.011.

51. Wen, H., Zhu, H., Xu, Y., Yan, B., Shutes, B., Bañuelos, G., Wang, X. (2021). Removal of sulfamethoxazole and tetracycline in constructed wetlands integrated with microbial fuel cells influenced by influent and operational conditions. *Environmental Pollution*, *272*, 115988. https://doi.org/10.1016/j.envpol.2020.115988.

52. Yaqoob, A.A., Ibrahim, M.N.M., Yaakop, A.S., Ahmad, A. (2021). Application of microbial fuel cells energized by oil palm trunk sap (OPTS) to remove the toxic metal from synthetic wastewater with generation of electricity. *Applied Nanoscience*, *11*, 1949–1961. https://doi.org/10.1007/s13204-021-01885-6.

53. Yaqoob, A.A., Al-Zaqri, N.,Alamzeb, M., Hussain, F., Oh, S.E., Umar, K. (2023). Bioenergy generation and phenol degradation through microbial fuel cells energized by domestic organic waste. *Molecules*, *28*, 4349. https://doi.org/10.3390/molecules28114349.

54. Yoon, K.J., Zink, P., Gopalan, S., Pal, U.B. (2007). Polarization measurements on single-step co-fired solid oxide fuel cells (SOFCs). *Journal of Power Sources*, *172*, 39–49. https://doi.org/10.1016/j.jpowsour.2007.03.003.